Envelope - Finite Element (EVFE) Technique in Electromagnetics with Perfectly Matched Layer (PML)

Weijun Yao, Yuanxun Wang, and Tatsuo Itoh

*Abstract — **In this paper, the perfectly matched layer (PML) has been implemented into the Envelope Finite Element (EVFE) technique. The PML performance tests show that it can provide sufficient absorption of the incident waves both in 2D and 3D cases. The 3D guided wave structures are efficiently analyzed by the EVFE technique with the PML boundary condition. Furthermore, a new plane wave excitation scheme inside the PML boundary with EVFE technique is also presented here for the analysis of scattering problems, and the numerical examples validate the formulations.***

I. INTRODUCTION

In modern optical and wireless communication systems, the digital modulated signals are usually further modulated with a very high frequency carrier, such that the signal bandwidth to carrier frequency ratio is very small. To analyze the transient response of the components and devices in this kind of system, the traditional time domain techniques are not efficient and precise enough. The reasons are: first, although we can develop implicit method to make the time domain algorithms unconditionally stable, such as implicit finite element time domain (FETD) method [1], the time step size is still governed by Nyquist sampling criterion, which requires that the sampling rate is at least twice of the simulation bandwidth. As the simulation bandwidth in FETD ranges from DC to the highest frequency of the narrowband modulated signal, the required time step should be very small in order to follow the variance of high frequency carrier. Second, as FETD is low pass type of algorithm, the time dispersion error is smallest at DC, and continually increases as frequency increases. This characteristic made traditional FETD unsuitable to simulate narrow band systems because its time dispersion will be very large at the carrier frequency [2].

Recently, a new numerical technique called envelope finite element was proposed in [2]-[5]. In this method, the carrier information is de-embedded from the narrowband signal thus only the complex signal envelopes are sampled. Its simulation bandwidth is much smaller compared with finite element time domain (FETD) method. Numerical tests in [2] shows, with same time step size, EVFE has a much lower time dispersion error than FETD. This is accomplished while, keeping the same time dispersion error, suggesting that EVFE can use much larger time step size than FETD. It can be asserted that EVFE is a powerful tool to simulate the transient response of components and devices in the narrowband system. The concept of envelope simulation itself is not new, which has been employed into the circuit simulator, such as ADS's Circuit Envelope Simulator [6]. It has been proven to be much more efficient than the regular transient simulator. EVFE technique makes it possible to do the efficient EM and circuit co-simulation combining with Circuit Envelope Simulator.

Previous researchers have already applied EVFE technique to 2-D guided wave problems [3] and 3-D microwave passive structures [4] with the first order absorbing boundary condition (ABC); however, an alternative and better choice to ABC is perfectly matched layer (PML) boundary condition, which has wider bandwidth and can provide more absorption of the incident waves. Perfectly matched layer was first introduced into finite difference time domain (FDTD) method by Berenger [7], however, it has several limitations such as the governing equation inside the PML region is non-Maxwellian. Sacks [8] has suggested a new PML based on a lossy uniaxial medium and successfully implemented into frequency domain finite element method. Gendey [9] further developed the formulation for the FDTD method with anisotropic perfectly matched layer and applied it in the analysis of microwave circuits and antennas. Recently, PML has been successfully implemented into finite element time domain technique (FETD) in the analysis of scattering problems [10], and active nonlinear microwave circuit modeling [11]. Based on the anisotropic PML concept, we derived the PML formulations for EVFE technique. Several numerical tests and examples will be shown to validate our formulations.

This paper is organized as follows. Section II presents the EVFE formulations for implementing the anisotropic perfectly matched layer and two examples are presented to test the PML's performance both in 2-D and 3-D. Section III presents 3-D examples for the analysis of guided wave structures with EVFE and PML technique. In section IV a

new plane wave excitation scheme inside the PML boundary is proposed and scattering problems are analyzed with this method. Finally, conclusions are made in section V.

II. PML FOR EVFE FORMULATIONS

In this section, the PML formulation will be derived for EVFE technique. To make the discussion more general, we present 3-D formulations here, which can be easily reduced to 2-D formulations. We would like to start from the general time-harmonic form of Maxwell equations in PML regions:

$$\nabla\times\vec{H} = j\omega\varepsilon_0\varepsilon_r\bar{\bar{\varepsilon}}\vec{E} + \vec{J}_i, \qquad \nabla\times\vec{E} = -j\omega\mu_0\mu_r\bar{\bar{\mu}}\vec{H}, \tag{1}$$

where

$$\bar{\bar{\varepsilon}} = \bar{\bar{\mu}} = \begin{bmatrix} \frac{s_y s_z}{s_x} & 0 & 0 \\ 0 & \frac{s_x s_z}{s_y} & 0 \\ 0 & 0 & \frac{s_x s_y}{s_z} \end{bmatrix} \tag{2}$$

and $s_i = 1 + \frac{\sigma_i}{j\omega\varepsilon_0},\ i = x, y, z$. (3)

Here we assume there is no source in PML region, and the second-order wave equation from (1), (2), and (3) is:

$$\nabla\times\left(\left[\bar{\bar{\mu}}\right]^{-1}\cdot\nabla\times\vec{E}\right) - \omega^2\varepsilon\left[\bar{\bar{\varepsilon}}\right]\vec{E} = -j\omega\frac{1}{\mu}\vec{J}. \tag{4}$$

Based on the vector finite element method, we can recast (4) into the following form

$$-\omega^2 e_j Q_x \frac{s_y s_z}{s_x} + e_j P_x \frac{s_x}{s_y s_z} - \omega^2 e_j Q_y \frac{s_x s_z}{s_y} + e_j P_y \frac{s_y}{s_x s_z}$$
$$-\omega^2 e_j Q_z \frac{s_y s_x}{s_z} + e_j P_z \frac{s_z}{s_y s_z} = -j\omega\int_v \frac{1}{\mu}\overrightarrow{N_i}\bullet\vec{J}dv, \tag{5}$$

where

$$Q_x = \int_v \varepsilon N_x^j N_x^i dv,$$
$$Q_y = \int_v \varepsilon N_y^j N_y^i dv,$$
$$Q_z = \int_v \varepsilon N_z^j N_z^i dv,$$
$$P_x = \int_v \frac{1}{\mu}(\nabla\times\vec{N}^j)_x(\nabla\times\vec{N}^j)_x dv,$$
$$P_y = \int_v \frac{1}{\mu}(\nabla\times\vec{N}^j)_y(\nabla\times\vec{N}^j)_y dv,$$
$$P_z = \int_v \frac{1}{\mu}(\nabla\times\vec{N}^j)_z(\nabla\times\vec{N}^j)_z dv, \tag{6}$$

while $\vec{N}^i, \vec{N}^j$ are the vector basis functions.

To solve equation (5), we need to define another three variables:

$$\Phi_x = \frac{s_x}{s_y s_z}e_j, \qquad \Phi_y = \frac{s_y}{s_x s_z}e_j, \qquad \Phi_z = \frac{s_z}{s_x s_z}e_j. \tag{7}$$

Equations (3)-(5) are reduced to

$$-\omega^2\Phi_z Q_x s_y^2 + P_x\Phi_x - \omega^2\Phi_x Q_y s_z^2 + P_y\Phi_y$$
$$-\omega^2\Phi_z Q_z s_x^2 + P_z\Phi_z = -j\omega\int_v \frac{1}{\mu}\overrightarrow{N}\bullet\vec{J}dv \tag{8}$$

and defining the signal envelope as

$$e_j(t) = u_j(t)e^{j\omega_c t},$$
$$\Phi_j(t) = \psi_j(t)e^{j\omega_c t},$$
$$J_z(t) = j_z(t)e^{j\omega_c t}. \tag{9}$$

Substituting (9) into (8) we can obtain the differential equation about the signal envelope

$$Q_x\frac{d^2\psi_z}{dt^2} + [S_1]\frac{d\psi_z}{dt} + [S_2]\psi_z + Q_y\frac{d^2\psi_x}{dt^2} +$$
$$[S_3]\frac{d\psi_x}{dt} + [S_4]\psi_x + Q_z\frac{d^2\psi_y}{dt^2} + [S_5]\frac{d\psi_y}{dt} +$$
$$[S_6]\psi_y = -(\frac{\partial f_i}{\partial t} + j\omega_c f_i) \tag{10}$$

where

$$S_1 = 2(j\omega_c + \frac{\sigma_y}{\varepsilon_0})Q_x, \qquad S_2 = (j\omega_c + \frac{\sigma_y}{\varepsilon_0})^2 Q_x + P_z,$$
$$S_3 = 2(j\omega_c + \frac{\sigma_z}{\varepsilon_0})Q_y, \qquad S_4 = (j\omega_c + \frac{\sigma_z}{\varepsilon_0})^2 Q_y + P_x,$$
$$S_6 = (j\omega_c + \frac{\sigma_x}{\varepsilon_0})^2 Q_z + P_y, \qquad S_5 = 2(j\omega_c + \frac{\sigma_x}{\varepsilon_0})Q_z,$$
$$f_i = \int_v \frac{1}{\mu}\overrightarrow{N_i}\bullet\vec{J}dv. \tag{11}$$

Using Newmark-Beta formulation to descretize (10), we can obtain the time recursive formulation

$$R_1\psi_z^{n+1} + R_2\psi_z^n + R_3\psi_z^{n-1} + R_4\psi_x^{n+1} + R_5\psi_x^n + R_6\psi_x^{n-1} + R_7\psi_y^{n+1} + R_8\psi_y^n + R_9\psi_y^{n-1} = -\left(\frac{f_i^{n+1} - f_i^{n-1}}{2\Delta t} + j\omega_c \frac{f_i^{n+1} + 2f_i^n + f_i^{n-1}}{4}\right) \quad (12)$$

where R_i are the coefficient matrixes. According to (7), we can obtain the relationship between the ψ_ξ (ξ=x,y,z) and u with Newmark-Beta formulation

$$\psi_\xi^{n+1} = a_{\xi 5}\psi_\xi^n + a_{\xi 6}\psi_\xi^{n-1} + a_{\xi 7}u^{n+1} + a_{\xi 8}u^n + a_{\xi 9}u^{n-1}, \quad (13)$$

where ξ=x,y,z and $a_{\xi i}$ are the complex coefficients. Combining equations (12) and (13), and solving them, the complex signal envelope vectors $u=[u_1,u_2,\ldots,u_N]$ and $\Psi_\xi = [\Psi_{\xi 1}, \Psi_{\xi 2},\ldots, \Psi_{\xi N}]$ can be solved in time domain.

In order to reduce the discretization error, we use spatially variant conductivity along the normal axis [7]

$$\sigma_z(z) = \frac{\sigma_{\max}\,|z - z_0|^m}{\sqrt{\varepsilon_r}\,d^m} \quad (14)$$

where z_0 is the interface between the PML region and non-PML region, d is the depth of the PML and m is the order the polynomial variation. The order m =2 is chosen for better absorption.

Two examples will be presented here to validate our EVFE formulations with PML boundary conditions. The first one is a 2-D example with the PML set at the end of a parallel waveguide. The incident modulated Guassian pulse's carrier frequency is 2.91 GHz and the excitation bandwidth is 0.8 GHz. The second example is a 3-D rectangle waveguide terminated with PML absorber. The crossection of the waveguide is 10.16 mm and 22.86 mm. The excitation's carrier frequency is about 10 GHz and the bandwidth is about 4 GHz.

Figs 1 and 2 show the results of PML tests. Both in 2-D and 3-D cases, PML can provide about -40dB absorption when four layers of PML are set. As the layers of PML increase, the absorption to the incident increases quickly.

III. WAVEGUIDE PROBLEM SOLUTION WITH THE 3-D EVFE AND PML

Two numerical examples will be shown here to verify the precision and efficiency of EVFE technique with PML. The first simulation structure is a rectangular waveguide with a dielectric post discontinuity shown in Fig. 3. The same geometry was analyzed by J-S Wang using FEM [12]. The waveguide has a width a = 22.86 mm (y-direction) and height b = 10.16 mm (x-direction). The dielectric slab has a height equal to that of the guide, width c = 12 mm, and length d = 6 mm. The relative dielectric constant of the slab is 8.2. In order to avoid the influence of the higher order modes, we set the observation point far enough from the discontinuity. TE_{10} mode is excited inside the waveguide with the center frequency 10 GHz and bandwidth 4 GHz. The excitation of EVFE in equation is represented as

$$J(t) = j(t)\, e^{j\omega_c t} = \exp\left[-\frac{(t - t_0)^2}{T^2}\right] e^{j\omega_c t} \quad (15)$$

where T = 4dt, t_0 = 12dt and dt = 25 ps.

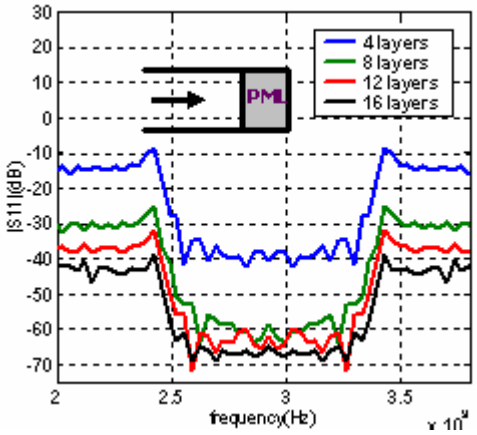

Fig. 1. Performance of PML for 2-D.

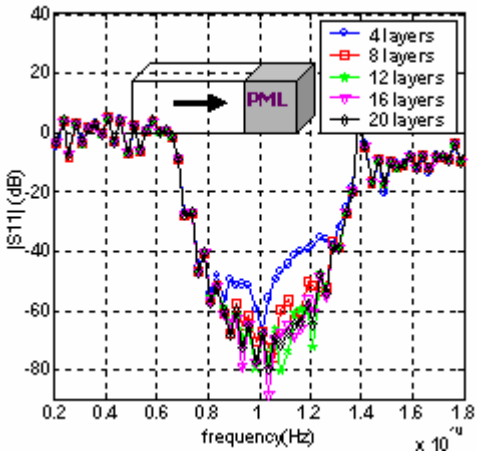

Fig. 2. Performance of PML for 3-D.

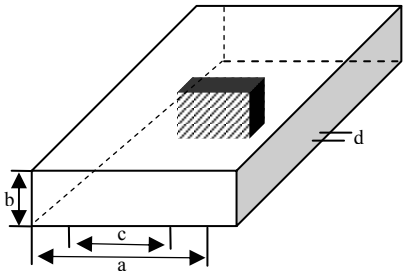

Fig. 3. Dielectric post discontinuity in a rectangular waveguide.

In FETD or FDTD case, CFL condition requires the time step to be less than 2ps. The total steps are about 12.5 times as many as what EVFE requires. In this example, 10 layers of PML are set at the each end of the waveguide.

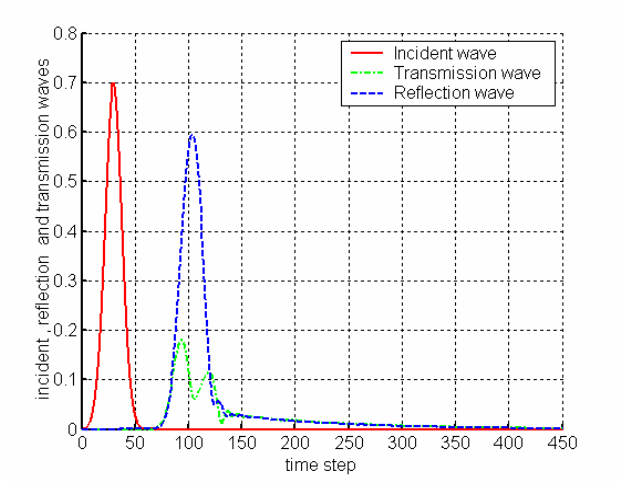

Fig. 4. Incident, reflection and transmission waves.

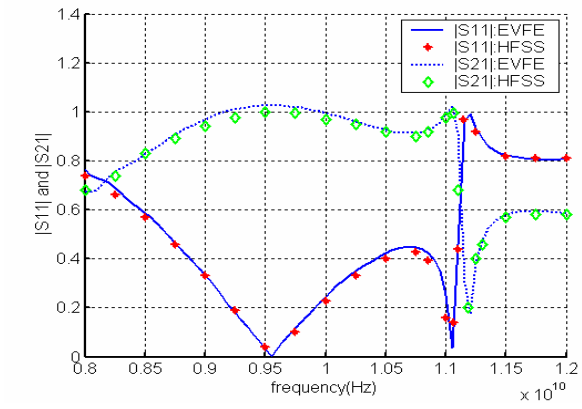

Fig. 5. Magnitudes of S_{11} and S_{21}.

Numerical Results for the time domain fields and magnitudes of S_{11} and S_{21} are shown in Fig. 4 and Fig. 5 respectively. The magnitudes of S_{11} and S_{21} are compared with the results calculated using HFSS, and they agree with each other very well.

The second example is a waveguide with a rectangle corner bend, filled with air, shown in Fig. 6. The waveguide has a width a = 20 mm and height b = 4 mm, with 10 layers PML set in two ends. In order to avoid the influence of the high order modes, we set the observation point far enough from the discontinuity. TE_{10} mode is excited inside the waveguide with a center frequency, f_c = 13 GHz and bandwidth Δf = 4 GHz. Numerical results of magnitudes of S_{11} and S_{21} are shown in Fig. 7. S_{11} and S_{21} are compared with the results calculated using HFSS, and they agree very well.

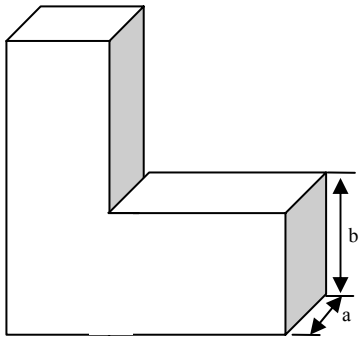

Fig. 6. Waveguide with right-angel corner band. a = 20 mm, b = 4 mm.

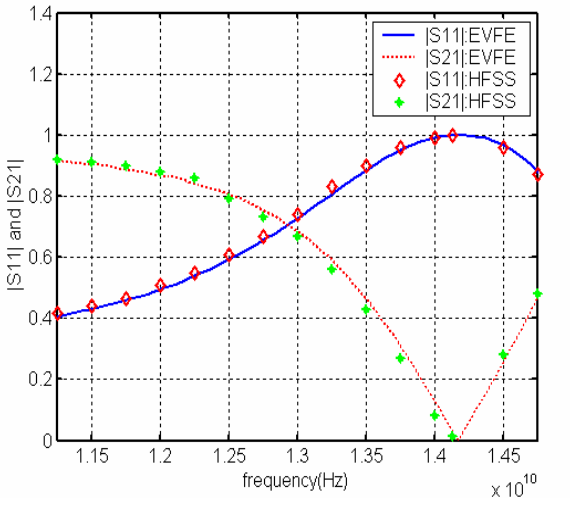

Fig. 7. Magnitudes of S_{11} and S_{21}.

IV. ANALYSIS OF 2-D SCATTERING PROBLEMS WITH EVFE & PML

Finite element methods have been extensively applied for scattering problem analysis with absorbing boundary conditions (ABCs). The plane wave excitation is straightforward for traditional Mur's ABCs. However, how to excite a plane wave in finite element analysis coupled with Perfect Matching Layer (PML) efficiently has not been thoroughly studied. In [13], a scattered field formulation is used for the entire computational domain. Therefore the applicability is limited for conductor only cases. In [10] and [14] the first effective approach addressing the excitation problem is proposed. The wave equation for the total field is used for the computational region while in PML region the incident field is switched to that in free space. To solve the unknown scattered field, however, it involves the updating of incident fields over the entire computational domain. Here, a simple and physically clear way to excite the plane wave is proposed based on the equivalence principle. The essential idea is to use both equivalent electric and magnetic currents on the virtual surface between these two regions. Though this concept has been well accepted for finite difference time domain (FDTD) simulations with PML [15], the implementation to the finite element approach has not been reported in literature yet. The main reason is that FEM is based on the single field (E-field) formulation, while both equivalent electric and magnetic currents need to be used to satisfy equivalence principle. In this paper, we shall present the implementation of the equivalence principle for plane wave incidence. With the proposed approach, this technique is applied to solve the scattering problems using finite element time domain (FETD) or envelope-finite element (EVFE) techniques, as the final performance of these techniques are strongly dependent on the perfect implementation of the PML boundary condition.

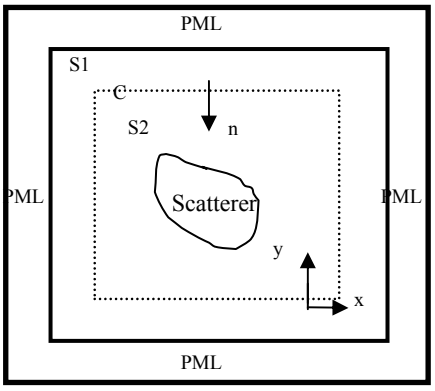

Fig. 8. Geometry of the 2-D scattering problem.

To derive the EVFE_PML formulations for the 2-D scattering problems, we start from the general wave equation in PML region

$$\nabla\times\left((\mu[\Lambda])^{-1}\cdot\nabla\times\vec{E}\right)-\omega^2\varepsilon[\Lambda]\vec{E}=0\cdot \tag{16}$$

This formulation can be extended to the whole computational area by defining $s_x=s_y=s_z=1$ in the non-PML region. Use testing function T to test the wave equation (16), we can obtain

$$\int_s\frac{\omega^2}{c^2}\varepsilon_r[\Lambda]\vec{E}Tds=\int_s T\nabla\times[(\mu_r[\Lambda])^{-1}\nabla\times\vec{E}]ds \tag{17}$$

where S is the surface of the whole 2-D computational domain. Defining an inner boundary C, S is separated into the inner region S_2 and outer region S_1, as shown in Fig. 8. It should be noted that the equivalent sources are placed on C and the inner boundary should be selected in the free space area enclosed by PML. Therefore, we represent the field in S_1 and S_2 by $\vec{E}^+$, $\vec{E}^-$ and $\vec{H}^+$, $\vec{H}^-$, Rewriting (17) in the region S_1 and S_2 yields,

$$\int_{s_1}\frac{\omega^2}{c^2}\varepsilon_r[\Lambda]\vec{E}^+Tds+\int_{s_1}\nabla T\times[(\mu_r[\Lambda])^{-1}\nabla\times\vec{E}^+]ds$$
$$-\oint_c T[\Lambda]^{-1}\nabla\times\vec{E}^+\bullet d\vec{l}=0. \tag{18}$$

$$\int_{s_2}\frac{\omega^2}{c^2}\varepsilon_r[\Lambda]\vec{E}^-Tds+\int_{s_2}\nabla T\times[(\mu_r[\Lambda])^{-1}\nabla\times\vec{E}^-]ds$$
$$-\oint_{-c} T[\Lambda]^{-1}\nabla\times\vec{E}^-\bullet d\vec{l}=0. \tag{19}$$

Furthermore, the field can be expanded using finite element basis functions by letting

$$T=N_i\ ,\qquad \vec{E}^{\pm}=\sum_{j=1}^{N}\hat{z}N_j e_j^{\pm}\ . \tag{20}$$

Substituting (1), (2), (20) into (18) and (19), for 2-D TM wave incidence, it yields

$$\sum_{j=1}^{N}\int_{s_1}\frac{\omega^2}{c^2}\varepsilon_r S_x S_y N_i N_j e_j^+ds-\sum_{j=1}^{N}e_j^+\int_{s_1}\frac{1}{\mu_r}\left[\frac{s_y}{s_x}\frac{\partial N_j}{\partial x}\frac{\partial N_i}{\partial x}+\frac{s_x}{s_y}\frac{\partial N_j}{\partial y}\frac{\partial N_i}{\partial y}\right]ds$$
$$-\oint_c N_i(-j\omega\mu_r\mu_0\overline{H}^+)\bullet d\vec{l}=0, \tag{21}$$

$$\sum_{j=1}^{N}\int_{s_2}\frac{\omega^2}{c^2}\varepsilon_r S_x S_y N_i N_j e_j^- ds-\sum_{j=1}^{N}e_j^-\int_{s_2}\frac{1}{\mu_r}\left[\frac{s_y}{s_x}\frac{\partial N_j}{\partial x}\frac{\partial N_i}{\partial x}+\frac{s_x}{s_y}\frac{\partial N_j}{\partial y}\frac{\partial N_i}{\partial y}\right]ds$$
$$-\oint_{-c}N_i(-j\omega\mu_r\mu_0\overline{H}^-)\bullet d\vec{l}=0. \tag{22}$$

Adding (21) and (22) together, we can obtain

$$\sum_{j=1}^{N}\int_{s_1+s_2}\frac{\omega^2}{c^2}\varepsilon_r S_x S_y N_i N_j e_j ds-\sum_{j=1}^{N}e_j\int_{s_1+s_2}\frac{1}{\mu_r}\left[\begin{array}{l}\frac{s_y}{s_x}\frac{\partial N_j}{\partial x}\frac{\partial N_i}{\partial x}\\+\frac{s_x}{s_y}\frac{\partial N_j}{\partial y}\frac{\partial N_i}{\partial y}\end{array}\right]ds$$
$$-\oint_c N_i[-j\omega\mu_r\mu_0(\overline{H}^+-\overline{H}^-)]\bullet d\vec{l}=0. \tag{23}$$

In (23), e represents e^+ inside region S_1 and e^- inside S_2.
The loop integral in (23) shows the contribution of the equivalent electric current on C. The relation between the fields in region 1 and region 2 can be expressed as

$$\vec{E}^+-\vec{E}^-=\vec{E}^{inc}, \tag{24}$$
$$\vec{H}^+-\vec{H}^-=\vec{H}^{inc}. \tag{25}$$

Because the electric field on the boundary C is not continuous due to the magnetic current excitation, it needs to be defined. Here we assume $e=e^-$ on C, thus e^+ unknowns on the excitation boundary can be eliminated by using (24). Substituting (24) and (25) into (23) yields a general equation for E fields

$$\sum_{j=1}^{N}e_j\int_s\frac{\omega^2}{c^2}\varepsilon_r S_x S_y N_i N_j ds-\sum_{j=1}^{N}e_j\int_s\frac{1}{\mu_r}\left[\begin{array}{l}\frac{s_y}{s_x}\frac{\partial N_j}{\partial x}\frac{\partial N_i}{\partial x}\\+\frac{s_x}{s_y}\frac{\partial N_j}{\partial y}\frac{\partial N_i}{\partial y}\end{array}\right]ds$$
$$=\oint_c N_i[-j\omega\mu_r\mu_0(H^{inc})]\bullet d\vec{l}-\sum_{j=1}^{N_1}\int_s\frac{\omega^2}{c^2}\varepsilon_r S_x S_y N_i N_j E_j^{inc}ds$$
$$+\sum_{j=1}^{N_1}E_j^{inc}\int_s\frac{1}{\mu_r}\left[\frac{s_y}{s_x}\frac{\partial N_j}{\partial x}\frac{\partial N_i}{\partial x}+\frac{s_x}{s_y}\frac{\partial N_j}{\partial y}\frac{\partial N_i}{\partial y}\right]ds. \tag{26}$$

In (26), both electric and magnetic currents are included in the right hand side. N_1 denotes the element numbering which are related with the excitation boundary C.
Thus we can obtain the matrix equation

$$-\frac{\omega^2}{c^2}s_x s_y e_j[A]+e_j\frac{s_x}{s_y}[B]+e_j\frac{s_y}{s_x}[C]$$
$$=j\omega\mu_0 f+\frac{\omega^2}{c^2}s_x s_y E_j^{inc}[A]-E_j^{inc}\frac{s_x}{s_y}[B]-E_j^{inc}\frac{s_y}{s_x}[C] \tag{27}$$

where

$$[A]_{ij}=\int_s\varepsilon_r N_i N_j ds,$$
$$[B]_{ij}=\int_s\frac{1}{\mu_r}\frac{\partial N_j}{\partial y}\frac{\partial N_i}{\partial y}ds,$$
$$[C]_{ij}=\int_s\frac{1}{\mu_r}\frac{\partial N_j}{\partial x}\frac{\partial N_i}{\partial x}ds,$$
$$[f]_i=\oint_c H^{inc}N_i\mu_r\cdot d\vec{l}.$$

Notice that E^{inc} is zero except on the excitation boundary C. The internal boundary integral terms inside PML vanish because of the continuity of tangential H field. If we define another variable Φ and Φ^{inc}

$$\Phi_j=e_j/(-\omega^2 s_x s_y)$$
and
$$\Phi_j^{inc}=E_j^{inc}/(-\omega^2 s_x s_y) \tag{28}$$

and substitute (28) into (27), we get

$$-\frac{\omega^2}{c^2}s_x s_y e_j[A]-\Phi_j\omega^2 s_x^2[B]-\Phi_j\omega^2 s_y^2[C]$$
$$=\frac{\omega^2}{c^2}s_x s_y E_j^{inc}[A]+\Phi_j^{inc}\omega^2 s_x^2[B]+\Phi_j^{inc}\omega^2 s_y^2[C]+j\omega\mu_0 f. \tag{29}$$

So far, (29) is the derived frequency domain wave equation in PML medium. A transformation is needed in order to change (29) to time/envelope domain. First we define the complex signal envelope of the fields as

$$e_j(t)=u_j(t)e^{j\omega_c t},\qquad \Phi_j(t)=\psi_j(t)e^{j\omega_c t},$$
$$e_j^{inc}(t)=u_j^{inc}(t)e^{j\omega_c t},\qquad J_z(t)=j_z(t)e^{j\omega_c t},$$
$$\Phi_j^{inc}(t)=\psi_j^{inc}(t)e^{j\omega_c t}, \tag{30}$$

where ω_c is the carrier frequency and u, ψ, j_z are the complex envelopes. Further incorporating the Fourier transform relationship between frequency domain and time domain, the transform between the frequency domain operators and envelope domain operators are:

$$j\omega\rightarrow\frac{\partial}{\partial t}e^{j\omega_c t}+j\omega_c e^{j\omega_c t}, \tag{31}$$
$$-\omega^2\rightarrow\frac{\partial}{\partial t^2}e^{j\omega_c t}+2j\omega_c\frac{\partial}{\partial t}e^{j\omega_c t}-\omega_c^2 e^{j\omega_c t}.$$

It is evident that setting ω_c as zero in the above formulas leads to the conventional Fourier transform. Therefore, (29) is converted into envelope domain:

$$[T_1]\frac{d^2u_j}{dt^2}+[T_2]\frac{du_j}{dt}+[T_3]u_j+[T_4]\frac{d^2\psi_j}{dt^2}+[T_5]\frac{d\psi_j}{dt}$$
$$+[T_6]\psi_j=\frac{\partial f}{\partial t}+[T_1]\frac{d^2u_j^{inc}}{dt^2}+[T_2]\frac{du_j^{inc}}{dt}+[T_3]u_j^{inc}$$
$$+[T_4]\frac{d^2\psi_j^{inc}}{dt^2}+[T_5]\frac{d\psi_j^{inc}}{dt}+[T_6]\psi_j^{inc}, \tag{32}$$

where

$$[T_1]_{ij}=\frac{[A]_{ij}}{c^2},$$
$$[T_2]_{ij}=\frac{[A]_{ij}}{c^2}\left(2j\omega_c+\frac{\sigma_x+\sigma_y}{\varepsilon_0}\right),$$
$$[T_3]_{ij}=\frac{[A]_{ij}}{c^2}\left(-\omega_c^2+j\omega_c\frac{\sigma_x+\sigma_y}{\varepsilon_0}+\frac{\sigma_x\sigma_y}{\varepsilon_0^2}\right),$$
$$[T_4]_{ij}=[B]_{ij}+[C]_{ij},$$
$$[T_5]_{ij}=2\left(j\omega_c+\frac{\sigma_x}{\varepsilon_0}\right)[B]_{ij}+2\left(j\omega_c+\frac{\sigma_y}{\varepsilon_0}\right)[C]_{ij},$$
$$[T_6]_{ij}=\left(j\omega_c+\frac{\sigma_x}{\varepsilon_0}\right)^2[B]_{ij}+\left(j\omega_c+\frac{\sigma_y}{\varepsilon_0}\right)^2[C]_{ij}. \tag{33}$$

For the same reason, equation (28) results in,

$$u_j^{inc}=\frac{\partial^2\psi_j^{inc}}{\partial t^2}+\left(2j\omega_c+\frac{\sigma_x+\sigma_y}{\varepsilon_0}\right)\frac{\partial\psi_j^{inc}}{\partial t}$$
$$+\left(-\omega_c^2+j\omega_c\frac{\sigma_x+\sigma_y}{\varepsilon_0}+\frac{\sigma_x\sigma_y}{\varepsilon_0^2}\right)\psi_j^{inc}.$$
$$u_j=\frac{\partial^2\psi_j}{\partial t^2}+\left(2j\omega_c+\frac{\sigma_x+\sigma_y}{\varepsilon_0}\right)\frac{\partial\psi_j}{\partial t}+\left(-\omega_c^2+j\omega_c\frac{\sigma_x+\sigma_y}{\varepsilon_0}+\frac{\sigma_x\sigma_y}{\varepsilon_0^2}\right)\psi_j. \tag{34}$$

Using Newmark-Beta formulations [3] to discretize (32) and (34) in time domain yields two difference equations. The "Mutual Difference" scheme [5] can then be used to solve these two equations jointly to update the complex signal envelope vector $u=[u_1,u_2,\ldots,u_N]$ and $\Psi=[\Psi_1,\Psi_2,\ldots,\Psi_N]$ in time.

Two numerical examples are presented to validate the proposed scheme. The scattering problem about the cylindrical perfect electric conductor (PEC) is first solved using EVFE technique. Here we define the incident plane wave in the form of modulated Gaussian pulse. For simplicity, we assume the incident wave impinges in x direction, and the carrier frequency is ω_c, the envelopes of the incident fields thus become

$$\vec{E}^{inc}=\hat{z}\exp\left(-\left[\frac{t-t_2-x/v}{t_1}\right]^2-j\omega_c x/v\right)$$

$$\vec{H}^{inc}=-\hat{y}\frac{1}{\mu}$$
$$\int\left(2\left[\frac{t-t_2-x/v}{vt_1^{\,2}}\right]-\frac{j\omega_c}{v}\right)\exp\left(-\left[\frac{t-t_2-x/v}{t_1}\right]^2-j\omega_c x/v\right)dt. \tag{35}$$

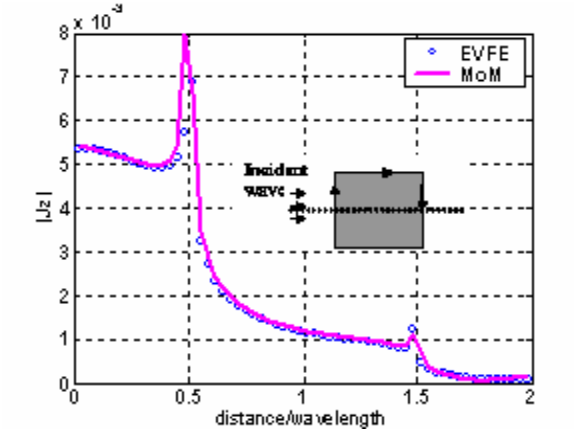

Fig.9. Magnitude of surface current on upper half cylinder at f=2 GHz.

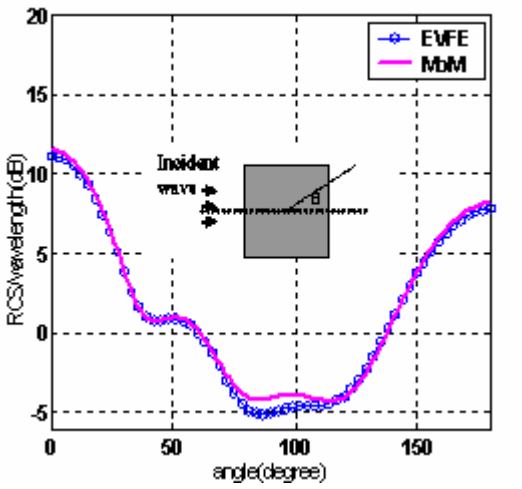

Fig.10. Normalized RCS of the cylinder in Fig. 9 at different observation angles at f=2 GHz.

Consider a perfectly conducting square cylinder with the side length 0.15 m. Six PML layers are set 2.5 cm away from the PEC cylinder's surface. The incidence wave is a modulated Gaussian pulse (35) with a center frequency 2 GHz and a bandwidth of 1 GHz. The polarization is TM. The excitation boundary C is only 1.5 cm away from the

PEC object and 1 cm away from the PML region. The result for the surface current on the upper half of the cylinder is plotted in Fig. 9, where the frequency is 2 GHz. The result of the normalized RCS is presented in Fig. 10. The results agree well with those obtained using Method of Moments (MoM).

Another example is a square two-dimensional homogeneous anisotropic dielectric scatterer. The scatterer to be simulated is a square anisotropic cylinder with ε_{zz}=1.5, μ_{xx}=1.5, μ_{yy}=3 and k_0s=10, where k_0 is set according to the center frequency of the Gaussian incident plane wave, and s is the side length of the square cylinder. In this case, the excitation boundary C is only $0.1\lambda_0$ away from the scatter and $0.1\lambda_0$ away from the ten layers PML region, where λ_0 is according to the center frequency. The result about the magnitude of the magnetic current on center frequency is plotted in Fig. 11 which agrees well with the result of FDTD [16].

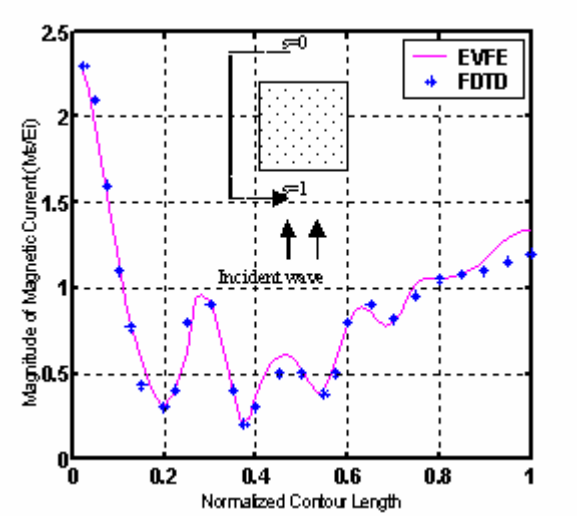

Fig. 11. Surface magnetic current distribution of square anisotropic cylinder with ε_{zz}=1.5, μ_{xx}=1.5, μ_{yy}=3 and k_0s=10.

V. CONCLUSION

In this paper, anisotropic PML has been implemented into the 2-D and 3-D EVFE formulations. Numerical examples have been presented to evaluate the PML's performance and about 40dB absorption is achieved when a 4-layer absorber is used in both 2-D and 3-D cases. The EVFE technique with PML is validated through the simulation of the guided wave structures. The new method for exciting a plane wave inside the PML boundary has been proposed and the numerical examples of scattering problems are also presented to show the validity of the formulations.

REFERENCE

[1] S. D. Gedney and U. Navsariwala, "An unconditionally stable finite element time-domain solution of the vector wave equation", *Microwave and Guided Wave Letters, IEEE [see also IEEE Microwave and Wireless Components Letters]*, pp. 332-334, Vol. 5, Issue: 10, Oct. 1995.

[2] W. Yao and Y. Wang, "Numeric Dispersion Analysis of 3D Envelope-Finite Element (EVFE) Method", *IEEE-Antenna and Propagation Symposium 2003, Columbus, Ohio.*

[3] Y. Wang and T. Itoh, "Envelope-finite element (EVFE) Technique – A more efficient time domain scheme", *IEEE Trans. Microwave Theory Tech*. Vol. 49, pp 2241 -2247, Dec. 2001.

[4] H. P. Tsai,Y. Wang and T. Itoh, "Efficient analysis of microwave passive structures using 3-D envelope-finite element (EVFE)", *IEEE Trans. Microwave Theory Tech.* Vol. 50. Issue: 12, pp. 2721 –2727, Dec. 2002.

[5] W. Yao and Y. Wang, "An Equivalence Principle Based Plane Wave Excitation in Time/Envelope Domain Finite Element Analysis", submitted to *IEEE - Antennas and Wireless Propagation Letters.*

[6] H. S. Yap, "Designing to digital wireless specifications using circuit envelope simulation," in *Asia–Pacific Microwave Conf.*, pp. 173–176, 1997.

[7] J. P. Berenger, "A perfectly matched layer for the absorption of electromagnetic waves," *J. Comput. Phys.*, Vol. 114, pp. 185–200, Oct. 1994.

[8] Z. S. Sacks, D. M. Kingsland, R. Lee, and J.-F. Lee, "A perfectly matched anisotropic absorber for use as an absorbing boundary condition," *IEEE Trans. Antennas Propagat.*, Vol. 43, pp. 1460–1463, Dec.1995.

[9] S.D. Gedney, "An Anisotropic Perfectly Matched Layer Absorbing Medium for the Truncation of FDTD Lattices," *IEEE Trans. Antennas Propagat.*, Vol.44, no.12, pp.1630-1639, Dec. 1993.

[10] D. Jiao, J. M. Jin, E. Michielssen and D. J. Riley "Time-Domain Finite-Element Simulation of Three-Dimensional Scattering and Radiation Problems Using Perfectly Matched Layers", *Trans. Antennas Propagat.*, Vol.51, (no.2), pp.296-305, Feb. 2003.

[11] H. P. Tsai, Y. Wang and T. Itoh, "An Unconditionally Stable Extended (USE) Finite Element Time Domain Solution of Active Nonlinear Microwave Circuits Using Perfectly Matched

Layers", *IEEE Trans. Microwave Theory Tech.*, pp 2226 –2232, Oct. 2002.

[12] J-S Wang and R. Mittra, "Finite Element Analysis of MMIC Structures and Electronic Packages Using Absorbing Boundary Conditions," *IEEE Trans. Microwave Theory and Tech*., Vol. 42, No. 3, pp. 441-449, Mar. 1994.

[13] D.M. Kingsland, J. Gong, J. L. Volakis and J.-F. Lee, "Performance of an anisotropic artificial absorber for truncating finite-element meshes", *IEEE Transactions on Antennas and Propagation* , Vol. 44, pp. 979 -981, July 1996.

[14] J. Jin, "The finite element method in electromagnetics", second edition, John Wiley & Sons. Inc, 2002.

[15] A. Taflove, "Computational electrodynamics– the finite-difference time-domain Method", Artech House, Inc, 1995.

[16] B. Beker, K. R. Umashankar and A. Taflove," Numerical analysis and validation of the combined field surface integral equations for electromagnetic scattering by arbitrary shaped two-dimensional anisotropic objects", *IEEE Trans. Antenna and Propagation.* Vol. 37, pp 1573-1581, Dec. 1989.

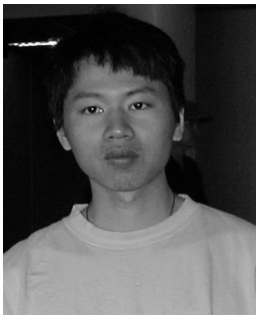

Weijun Yao received the B.S. degree in electrical engineering from University of Science and Technology of China (USTC), China in 2001 and M.S degree in electrical engineering department from University of California, Los Angeles in 2003. He is currently a Ph.D student in the department of electrical engineering in University of California, Los Angeles. His research interest includes smart antenna system design, UWB system design, and numeric modeling of microwave circuits and antenna.

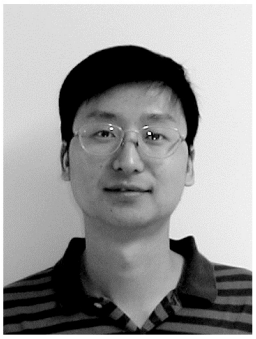

Yuanxun Wang received the B.S. degree in electrical engineering from University of Science and Technology of China (USTC), Hefei, in 1993, the M.S. and the Ph.D. degrees in electrical engineering from University of Texas at Austin, in 1996 and 1999. From 1995 to 1999, he worked as a Research Assistant in the Department of Electrical and Computer Engineering, University of Texas at Austin.

From 1999 to 2002, he worked as a research engineer and lecturer, in the Department of Electrical Engineering, University of California at Los Angeles (UCLA), prior to joining the faculty. He is an assistant professor in Electrical Engineering Department since 2002. His work is focused on high performance antenna array and microwave amplifier systems for wireless communication and radar, as well as numerical modeling techniques. His current research interests feature the fusion of signal processing and circuit techniques in microwave system design. He is a member of IEEE and SPIE. He has authored and coauthored over 60 refereed journal and conference papers.

Tatsuo Itoh received the Ph.D. Degree in Electrical Engineering from the University of Illinois, Urbana in 1969.

From September 1966 to April 1976, he was with the Electrical Engineering Department, University of Illinois. From April 1976 to August 1977, he was a Senior Research Engineer in the Radio Physics Laboratory, SRI International, Menlo Park, CA. From August 1977 to June 1978, he was an Associate Professor at the University of Kentucky, Lexington. In July 1978, he joined the faculty at The University of Texas at Austin, where he became a Professor of Electrical Engineering in 1981 and Director of the Electrical Engineering Research Laboratory in 1984. During the summer of 1979, he was a guest researcher at AEG-Telefunken, Ulm, West Germany. In September 1983, he was selected to hold the Hayden Head Centennial Professorship of Engineering at The University of Texas. In September 1984, he was appointed Associate Chairman for Research and Planning of the Electrical and Computer Engineering Department at The University of Texas. In January 1991, he joined the University of California, Los Angeles as Professor of Electrical Engineering and holder of the TRW Endowed Chair in Microwave and Millimeter Wave Electronics. He was an Honorary Visiting Professor at Nanjing Institute of Technology, China and at Japan Defense Academy. In April 1994, he was appointed as Adjunct Research Officer for Communications Research Laboratory, Ministry of Post and Telecommunication, Japan. He currently holds Visiting Professorship at University of Leeds, United Kingdom. He received a number of awards including Shida Award from Japanese

Ministry of Post and Telecommunications in 1998, Japan Microwave Prize in 1998, IEEE Third Millennium Medal in 2000, and IEEE MTT Distinguished Educator Award in 2000. He was elected to a member of National Academy of Engineering in 2003. Dr. Itoh is a Fellow of the IEEE, a member of the Institute of Electronics and Communication Engineers of Japan, and Commissions B and D of USNC/URSI. He served as the Editor of IEEE Transactions on Microwave Theory and Techniques for 1983-1985. He serves on the Administrative Committee of IEEE Microwave Theory and Techniques Society. He was Vice President of the Microwave Theory and Techniques Society in 1989 and President in 1990. He was the Editor-in-Chief of IEEE Microwave and Guided Wave Letters from 1991 through 1994. He was elected as an Honorary Life Member of MTT Society in 1994. He was the Chairman of\ USNC/URSI Commission D from 1988 to 1990, and Chairman of Commission D of the International URSI for 1993-1996. He is Chair of Long Range Planning Committee of URSI. He serves on advisory boards and committees of a number of organizations.

He has 310 journal publications, 640 refereed conference presentations and has written 30 books/book chapters in the area of microwaves, millimeter-waves, antennas and numerical electromagnetics. He generated 60 Ph.D. students.